Performance Analysis of Hybrid Interference Subspace Rejection in Multi-Rate CDMA

Besma Smida, Sofiène Affes, and Paul Mermelstein
INRS-EMT, Université du Québec
Place Bonaventure, 800, de la Gauchetière Ouest, Suite 6900
Montréal, Québec, H5A 1K6, Canada

***Abstract*— An efficient multiuser detection technique, denoted hybrid interference subspace rejection (ISR), has been recently developed for multi-rate CDMA transmissions with mixed spreading factors and/or modulations (as well as multi-code). In this paper, we derive a link/system-level performance analysis of hybrid ISR based on the Gaussian assumption (GA) and validate it by simulations. In addition, we design an efficient strategy for hybrid ISR, well adapted to multi-rate CDMA transmission, that strives to maximize throughput while containing the extra computational cost.**

I. Introduction

The "third-generation and beyond" wireless communication systems must be able to offer wireless transport for a variety of information sources with inherently different data rates, including data, image, and voice. In such mixed-rate traffic scenarios, the conventional receiver fails to demodulate transmissions from the weak low-rate users. It is therefore imperative to develop effective multi-rate code division multiple access (CDMA) multiuser detectors.

An efficient multiuser detection technique, denoted hybrid interference subspace rejection (ISR), first proposed for single-rate DS-CDMA [1], has been recently developed for multi-rate transmissions with mixed spreading factors and/or modulations (as well as multi-code) [2]. Indeed, single-rate ISR offers different modes (referred to as canonic in the following). Each canonic mode characterizes the interference vector in a different way and accordingly suppresses it. The TR (total realizations) mode nulls the total interference vector and hence requires accurate estimation of all the channel and data parameters of the *NI* interferers. The R (realizations) mode nulls the signal vector of each interferer and hence is not sensitive to power estimation errors. The D (diversities) mode nulls the signal vector from each interfering finger and hence gains additional robustness to channel estimation errors. The H (hypotheses) mode nulls the signal vector from each interfering symbol of each interferer and hence introduces robustness to symbol data estimation errors.

In multi-rate transmissions, however, low-rate users require increased protection from the strong interference of high-rate users. Unfortunately the simplest canonic mode is unable to provide adequate protection and a potential upgrade to more robust modes will note only increase the complexity but also results in more severe noise enhancement. Hybrid ISR exploits the performance-complexity tradeoffs between the different ISR canonic modes. Instead of detecting all active users targeted for suppression with the same canonic ISR mode, hybrid ISR splits them into several groups based on their data rate, then applies different canonic ISR modes for their nulling, the number of nulling constraints being larger for groups with higher transmission rates. The performance of hybrid ISR was evaluated through simulations using very realistic link-level simulation setups [2]. Simulation results confirm the improved complexity/performance tradeoffs provided by hybrid ISR.

In this paper, we develop a theoretical link/system-level performance analysis of hybrid ISR based on the Gaussian assumption (GA), under the condition of realistic wireless transmission that takes into account frequency mismatch, imperfect power control and channel identification errors. We validate the Gaussian approximation (GA) of the interference by comparison with simulation results. In addition, we design an efficient strategy for hybrid ISR, well adapted to multi-rate CDMA transmission, that strives to maximize throughput while containing the extra computational cost.

II. Multi-Rate CDMA Data Model

We consider the uplink of an asynchronous multi-cellular multi-rate CDMA system where each base station is equipped with M receiving antennas. The system consists of U in-cell active users that transmit data with different spreading factors and different modulation formats (extension to the multi-code scheme is *ad hoc*). The data $b_n^u \in C_{\mathcal{M}_u}$ for a user assigned the index u is $\mathcal{M}_u$-PSK modulated and differentially[1] encoded at rate $1/T_u$, where T_u is the symbol duration and $C_{\mathcal{M}_u} = \{\ldots, e^{\frac{j2\pi m}{\mathcal{M}_u}}, \ldots\}$, $m \in \{0, \ldots, \mathcal{M}_u - 1\}$. The data sequence is then spread by a long spreading code $c^u(t)$. The spreading factor L_u is defined as the ratio of the symbol duration T_u and the chip duration T_c. We convert the variable spreading factor scenario into a single spreading factor scenario where each high data-rate user is equivalent to Q_u virtual low data-rate users. Regardless of the data-rate, the receiver implements down conversion, matched pulse filtering and chip-rate sampling followed by framing the observation into overlapping blocks of constant length of N_P chips. The resulting processing block duration $T_P = N_P T_c$ is equal to $T_{max} + \overline{\Delta\tau}$. The processing period $T_{max} = Q_u T_u$, which is also equal to the maximum spreading factor L_{max} times T_c, contains integer numbers of symbols Q_u targeted for detection in each block for user u. The frame overlap $\overline{\Delta\tau} < T_{max}$, which is larger then the delay spread to allow multipath tracking [5], comprises $Q_{\overline{\Delta},u} = \lceil \overline{\Delta\tau}/T_u \rceil$ symbols for user u. Hence we obtain the $M \times N_P$ matched-filter observation matrix [1]:

$$\mathbf{Y}_n = \sum_{u=1}^{U} \psi_n^u \mathbf{Y}_n^u + \mathbf{N}_n^{th}, \qquad (1)$$

where each user u contributes its user-observation matrix $\mathbf{Y}_n^u$ scaled by its total received power $(\psi_n^u)^2$ and where the base-band preprocessed thermal noise contributes $\mathbf{N}_n^{th}$. In the following, we assume that the base station targets *NI*

Work supported by a Canada Research Chair in High-Speed Wireless Communications and the Strategic Grants Program of NSERC.

[1] We can also use pilot symbols for coherent modulation and detection [6], but that is beyond the scope of this paper.

interfering users (presumably with high data-rate and/or strong power) for joint suppression among the U active users (*e.g.*, all incell users). Using Eq. (1) and defining a vector $\underline{V}$ as matrix $\mathbf{V}$ reshaped columwise, we can rewrite the matched-filtering observation matrix for the desired user assigned index $d \in \{1, \ldots NI\}$ with respect to its kth symbol targeted for detection for $k = 0, \ldots, Q_d - 1$ in the following vector form [1]:

$$\underline{Y}_n = \underbrace{s_n^{d,k} \underline{Y}_{k,n}^d}_{\text{desired signal}} + \underbrace{\sum_{\substack{i=1 \\ i \neq d}}^{NI} \psi_n^i \underline{Y}_n^i}_{\underline{I}_{\text{MAI},n}^d} + \underbrace{\sum_{\substack{k'=-Q_{\overline{\Delta},d} \\ k' \neq k}}^{Q_d + Q_{\overline{\Delta},d} - 1} s_n^{d,k'} \underline{Y}_{k',n}^d}_{\underline{I}_{\text{ISI},n}^{d,k}} + \underline{N}_n, \quad (2)$$

$$= s_n^{d,k} \underline{Y}_{k,n}^d + \underline{I}_n^{d,k} + \underline{N}_n, \quad (3)$$

where $s_n^{d,k} = \psi_n^d b_{k,n}^d$ is the kth signal component and $\underline{Y}_{k,n}^d$ is the canonic user-observation vector due to the k-th symbol. $\underline{I}_{\text{MAI},n}^d$ and $\underline{I}_{\text{ISI},n}^{d,k}$ are the multiple access interference and the inter-symbol interference to be suppressed with the respect to the kth symbol of user d. The noise vector $\underline{N}_n$ comprises the preprocessed thermal noise and the rest of the active users.

III. Hybrid ISR Performance Evaluation

This section is dedicated to the performance analysis of hybrid ISR. We exploit the analysis results of ISR recently developed in [3] at the link-level and extend them to hybrid ISR. Additionally, we broaden the scope of the analysis to include frequency mismatch, channel identification errors and imperfect power control [4]. We also provide a simple procedure to evaluate the capacity in terms of number of users per cell and the total system throughput.

A. Link-Level Performance Analysis

The signal after hybrid ISR combining is:

$$\begin{aligned} \widehat{s}_n^{d,k} &= \underline{W}_n^{d,k^H} \underline{Y}_n \\ &= \frac{\underline{\widehat{Y}}_{k,n}^{d\ H} \underline{Y}_{k,n}^d}{\|\underline{\widehat{Y}}_{k,n}^d\|^2} s_n^{d,k} + \delta_{MAI,n}^{d,k} + \delta_{ISI,n}^{d,k} + \underline{W}_n^{d,k^H} \underline{N}_n, \end{aligned} \quad (4)$$

where $\delta_{MAI,n}^{d,k}$ is the residual MAI and $\delta_{ISI,n}^{d,k}$ is the residual ISI. The hybrid ISR combiner $\underline{W}_n^{d,k}$ satisfies:

$$\begin{cases} \underline{W}_n^{d,k^H} \underline{\widehat{Y}}_{k,n}^d &= 1, \\ \underline{W}_n^{d,k^H} \widehat{\mathbf{C}}_n^{d,k} &= 0. \end{cases} \quad (5)$$

These constraints allow to derive the variance of the interference rejection residuals. The residual interferences are approximated as a Gaussian distributed random variable with zero mean. Only their variance needs to be evaluated. We define $E[\|\underline{W}_n^{d,k}\|^2] = \overline{\kappa}$ as a measure of the enhancement of the white noise compared to MRC ($\overline{\kappa} = 1$ for MRC) [3]. We exploit the expression of the variance of the channel identification error in [6] and the variance of the power control error in [4]. Let $\overline{\psi}_d^2 = E[(\psi^d)^2]$ be the average power of the the desired user and $\overline{\psi}_i^2$ be the average interference power of user i which varies with the spreading factor and modulation format. The variances of the residual MAI interferences can be written as:

$$\text{Var}[\delta_{MAI,n}^{d,k}] = \frac{1}{L_d} \sum_{\substack{i=1 \\ i \neq d}}^{NI} I(\overline{\psi}_i^2, m_i). \quad (6)$$

The interference term $I(\overline{\psi}_i^2, m_i)$ from user i depends on the power of the interferer as well as the canonic suppression mode m_i applied to this user:

$$\begin{cases} \overline{\psi}_i^2 \overline{\kappa}, & m_i = \text{MRC} \\ \overline{\psi}_i^2 \overline{\kappa}[(1 + \rho_\beta(f_D + \Delta f))(1 + \rho_\lambda(f_D + \Delta f))] & \\ -\overline{\psi}_i^2 \overline{\kappa}[\rho_\xi^{TR}(f_D + \Delta f)], & m_i = \text{TR} \\ \overline{\psi}_i^2 \overline{\kappa}[(1 + \rho_\beta(f_D)) - \rho_\xi^R(f_D)], & m_i = \text{R} \\ \overline{\psi}_i^2 \overline{\kappa}[1 - \rho_\xi^D], & m_i = \text{D} \\ \overline{\psi}_i^2 \overline{\kappa}[(1 + \rho_\beta(f_D)) - 1], & m_i = \text{H} \\ 0, & m_i = \text{HD} \end{cases} \quad (7)$$

where f_D and Δf are the maximum Doppler frequency and the carrier frequency offset, respectively. The detailed expressions of $\rho_\beta(f)$, ρ_λ, $\rho_\xi^{TR}(f)$, $\rho_\xi^R(f)$ and ρ_ξ^D are derived for a Rayleigh fading channel with P equal-power paths to yield:

$$\begin{aligned} \rho_\beta(f) &= \frac{P\mu\left(\overline{\kappa}\sigma_N^2 + \text{Var}[\delta_{\text{MAI},k,n}^d] + \text{Var}[\delta_{\text{ISI},k,n}^d]\right)}{2(1 - \frac{\mu\overline{\psi}_i^2}{2})} \\ &\quad + 2\left[1 - \mathcal{B}_0\left(\frac{2\pi f T_i}{\mu\overline{\psi}_i^2}\right)\right], \\ \rho_\lambda(f) &= \frac{4\pi^2(f_D \times PC_D)^2}{P-1}, \end{aligned} \quad (8)$$

and

$$\begin{aligned} \rho_\xi^{TR}(f) &= \frac{\rho_\xi\left[MP(NI-1)(Q_i + 2Q_{\overline{\Delta},i} + 1) + (1 + \rho_\lambda(f))(MP-1)(Q_i + 2Q_{\overline{\Delta},i})\right]}{NIMP(Q_i + 2Q_{\overline{\Delta},i} + 1) - 1} \\ &\quad + \frac{\rho_\xi\left[(1 + \rho_\lambda(f))(1 + \rho_\beta(f))(Q_i + 2Q_{\overline{\Delta},i})\right] + (1 + \rho_\lambda(f))(MP-1)}{NIMP(Q_i + 2Q_{\overline{\Delta},i} + 1) - 1}, \\ \rho_\xi^R(f) &= \frac{\rho_\xi\left[(MP-1)(Q_i + 2Q_{\overline{\Delta},i}) + (1 + \rho_\beta(f))(Q_i + 2Q_{\overline{\Delta},i})\right] + MP - 1}{MP(Q_i + 2Q_{\overline{\Delta},i} + 1) - 1}, \\ \rho_\xi^D &= \frac{\rho_\xi\left[MP(Q_i + 2Q_{\overline{\Delta},i})\right] + MP - 1}{MP(Q_i + 2Q_{\overline{\Delta},i} + 1) - 1}, \end{aligned} \quad (9)$$

where

$$\rho_\xi = (1 - (1 - \cos(2\pi/\mathcal{M}_i)) S_{MRC}^i)^2, \quad (10)$$

μ is the channel identification adaptation step-size, $\mathcal{B}_0$ is the Bessel function of the first kind of order 0, PC_D is the power control feedback delay and S_{MRC}^i is the symbol error rate after the MRC stage. It follows from Eq. (8) that $\rho_\beta(f)$ is dependent on the noise and residual interference variance. Due to the analytical complexity of the problem, we have resorted to a worst case analysis in which we have $\text{Var}[\delta_{\text{MAI},k,n}^d] + \text{Var}[\delta_{\text{ISI},k,n}^d] = \frac{\overline{\kappa}}{L_d} \sum_{\substack{i=1 \\ i \neq d}}^{NI} \overline{\psi}_i^2$. This is the same as assuming that all the users are detected by simple MRC, and hence the gains due to interference rejection are not taken into account when evaluating the channel identification error. The variances of the residual ISI interferences can be written as:

$$\text{Var}[\delta_{ISI,n}^{d,k}] = I(\overline{\psi}_d^2, m_d)(\overline{\kappa} - 1 + \delta_{is})/\overline{\kappa}, \quad (11)$$

where $\delta_{is} (0 \leq \delta_{is} < 1)$ is a measure of the relative impact of the interference generated by the other paths on a given path of the desired user [3]. The SNR of the desired user can be estimated as:

$$\text{SNR}_{ISR}^d = \frac{M\overline{\psi}_d^2}{\text{Var}[\delta_{\text{MAI},k,n}^d] + \text{Var}[\delta_{\text{ISI},k,n}^d] + \overline{\kappa}\sigma_N^2}. \quad (12)$$

1. Initialize capacity C=max$\{1/r_g\}$, $g \in \{1,\ldots,G\}$
2. Start computation loop:
2.1 Increment capacity C=C+0.1
2.2 For each group of users $g \in \{1,\ldots,G\}$
2.2.1 Compute the SNR with MRC
$SNR^g_{MRC} = \frac{M\overline{\psi}^2_g}{\frac{1}{L_g}\sum_{\substack{i=1\\i\neq g}}^G Cr_i\overline{\psi}^2_i + \frac{1}{L_g}(Cr_g-1)\overline{\psi}^2_g + f\frac{1}{L_g}\sum_{i=1}^G Cr_i\overline{\psi}^2_i}$
2.2.2 Compute the symbol error rate SER after MRC stage
$S^g_{MRC} = \Omega(\mathrm{SNR}^g_{MRC})$
2.2.3 Compute $\beta^2(f), \rho_\beta(f), \rho_\lambda(f), I(\overline{\psi}^2_g, m_g)$
2.2.4 Compute the SNR
$SNR^g_{ISR} = \frac{M\overline{\psi}^2_g}{\sum_{\substack{i=1\\i\neq g}}^G \frac{Cr_i I(\overline{\psi}^2_i, m_i)}{L_g} + \frac{(Cr_g-1)I(\overline{\psi}^2_g, m_g)}{L_g} + \overline{\kappa} f \sum_{i=1}^G \frac{Cr_i\overline{\psi}^2_i}{L_g}}$
2.3 if for $\forall g \in \{1,\ldots,G\}$, $SNR^g_{ISR} > SNR^G_{req}$ goto 2.1, else exit
3. Decrement capacity C=C-0.1

TABLE I

CAPACITY COMPUTATION PROCEDURE.

The BER performance of the d-th user's hybrid ISR receiver is then given as follows:

$$P^d_e = \Omega(\mathrm{SNR}^d_{ISR}), \tag{13}$$

where Ω represents the single-user bound (SUB), which is classically defined as a conditional Gaussian Q-function over ψ_d and ψ_i. When using this classical representation, the average BER is derived by first finding the pdfs of ψ_d and ψ_i and then averaging over those pdfs. Since it is difficult to find a simple expression for the pdfs of ψ_d and ψ_i, we may consider an approximative pdf. In this analysis, we choose to simulate Ω without imposing any pdf approximation.

The link-level performance analysis leads to a fundamental insight into the hybrid ISR mechanisms. It shows that hybrid ISR performance varies from user to user and depends on a wide variety of factors such as the detection mode, the propagation environment (data, channel, and power control estimation errors), and the strength of the background noise. It also confirms that the number of nulling constraints should be larger for the groups of users that generate higher transmission powers in order to improve the overall performance of the multi-rate system.

B. System-Level Performance Analysis

Using the link-level performance analysis established earlier, we propose a simple computation procedure to evaluate the capacity in terms of number of users per cell for a specific operating condition and mode assignment. The capacity evaluation procedure provides a classification of the different mode assignments at specific operating conditions. We translate the link-level results into system-level results in terms of total throughput (or spectrum efficiency) under the following four assumptions: 1) All the cells have the same average load of C users per cell. 2) All the cells have the same multi-rate distribution: The C users are divided into G groups, the proportion of users in the group g is denoted r_g (i.e. $\sum_{g=1}^G r_g = 1$). 3) Within each group g, all users are received with equal power denoted $\overline{\psi}^2_g$ (i.e., perfect PC). 4) The out-cell to in-cell interference ratio f is set to 0.3 [7]. Given these assumptions in an interference-limited system (noise is low compared to interference), the link-level SNR of the users in the g-th group (ignoring ISI for simplicity) is:

$$SNR^g_{ISR} = \frac{M\overline{\psi}^2_g}{\sum_{\substack{i=1\\i\neq g}}^G \frac{Cr_i I(\overline{\psi}^2_i, m_i)}{L_g} + \frac{(Cr_g-1)I(\overline{\psi}^2_g, m_g)}{L_g} + \overline{\kappa} f \sum_{i=1}^G \frac{Cr_i\overline{\psi}^2_i}{L_g}}. \tag{14}$$

The maximum number of users that can access the system can be hence calculated by the simple procedure illustrated in Tab. I. For a specific operating condition and mode assignment, the capacity evaluation procedure computes the link-level SNR for all groups of users. In a multi-rate system, each group of users has its own required SNR. The quality of service (QoS) constraints on the capacity become:

$$\forall g \in \{1,\ldots,G\}, \quad SNR^g_{ISR} \geq SNR^g_{req}, \tag{15}$$

where SNR^g_{req} is the required SNR derived from link-level simulations to meet a BER of 5% in order to achieve a QoS of 10^{-6} after channel decoding. After initialization, this procedure increments the capacity C, until the SNR^g_{ISR} given by Eq. (14) no longer exceeds the required SNR^g_{req}. C is then reduced to the largest value for which $\forall g \in \{1,\ldots,G\}$, $SNR^g_{ISR} \geq SNR^g_{req}$. In step 2.2.1, we use the fact that in each group g, all users are received with equal power denoted $\overline{\psi}^2_g$. Hence, the in-cell interference powers before despreading resulting from the $C-1$ in-cell users are $\sum_{\substack{i=1\\i\neq g}}^G Cr_i\overline{\psi}^2_i + (Cr_g-1)\overline{\psi}^2_g$. Assuming that the out-cell to in-cell interference ratio is f, the total received interference before despreading is $\sum_{\substack{i=1\\i\neq g}}^G Cr_i\overline{\psi}^2_i + (Cr_g-1)\overline{\psi}^2_g + f\sum_{i=1}^G Cr_i\overline{\psi}^2_i$. The total interference power is then reduced by the processing gain L_g. In step 2.2.2, we evaluate the symbol error rate S^d_{MRC} after the MRC stage as follows:

$$S^g_{MRC} = \Omega(\mathrm{SNR}^g_{MRC}), \tag{16}$$

where Ω represents the single-user bound (SUB). In step 2.2.3, $\varphi_\beta(f)$ is computed assuming the worst case of noise and residual interference variance. But the step-size μ is optimized at the operating conditions so as to minimize channel identification errors [6]. Thus, the capacity is optimized over μ. This procedure provides a simple performance evaluation tool for each mode assignment, which allows a quick selection of the best hybrid ISR mode assignments at specific operating conditions.

IV. SIMULATIONS AND CONCLUSIONS

We consider the uplink of a WCDMA base-station with $M = 2$ antennas operating at a chip rate of 3.840 Mcps and a carrier frequency of 1.9 GHz. The Rayleigh fading channel is frequency selective with $P = 3$ equal-power paths and a Doppler shift of 8Hz (*i.e.*, speed of 5 Km/h). We assume a linear delay drift of 0.07 ppm for each path. We implement closed-loop power control operating at 1600 Hz and adjusting the power in steps of ± 0.5 dB. An error rate on the power control bit of 5% and a feedback delay of $PC_D = 0.625$ ms are simulated. All the channel parameters, varying in time, are estimated by the spatio-temporal array-receiver (STAR) [5].

For validation purposes, we consider a dual-rate system and the combination of the TR and R, D, or H modes in hybrid

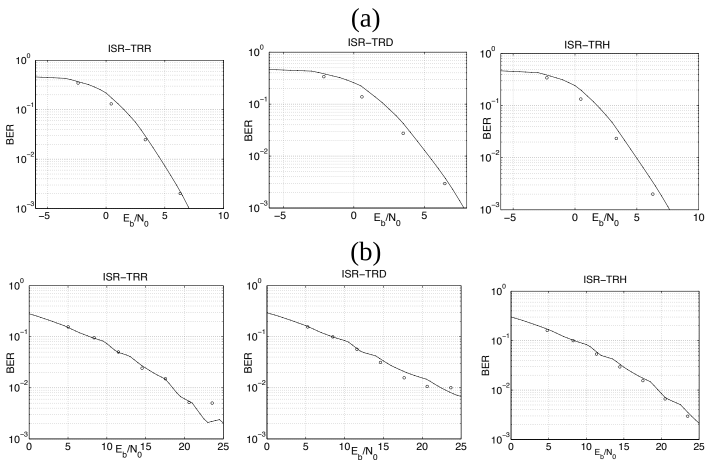

Fig. 1. BER vs SNR in dB with hybrid ISR (TR/R, TR/D, and TR/H) for (a): BPSK, (b): 8PSK.

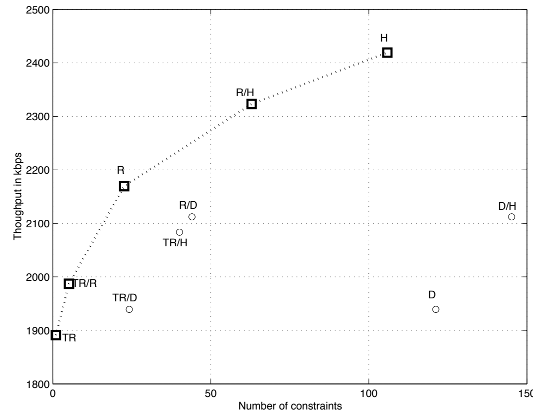

Fig. 2. The total throughput versus the number of constraints for the different mode assignments in dual-rate environment.

ISR. We also assume a frequency offset $\Delta f = 200$ Hz (*i.e.*, about 0.1 ppm). All users targeted for suppression are split into two groups, a larger number of N_l users with low data-rate and a smaller number of N_h users with high data-rate. The hybrid TR/R, TR/D, and TR/H modes null the low data-rate groups with the canonic TR mode. The hybrid TR/R, TR/D and TR/H null the high data-rate users with the canonic R, D and H modes, respectively. The multi-rate environment is simulated with $N_l = 10$ BPSK users and $N_h = 5$ 8PSK users with spreading factors of $L = 128$ and $L = 32$, corresponding to transmission rates of 30 Kb/s and 360 Kb/s, respectively. In Fig. 1-(a)(b), we plot the link-level performance of both BPSK and 8PSK users with the hybrid TR/R, TR/D, and TR/H modes. It is seen that there is in general a good match between analytical (plotted with solid line) and simulation (plotted with circles) results. We notice, however, that the analytical evaluation is less accurate for BPSK users with the TR/H mode because we overestimate the effect of the residual interference on the channel identification error. This approximation is even less accurate with low background noise and high residual interference.

In the following, we compare the performance of the different mode assignments. First, we select the operating conditions (i.e., speed= 100 Km/h, $\Delta f = 0$ Hz and data-rate distribution: 80% BPSK users and 20% 8PSK users with spreading factors of $L = 128$ and $L = 32$). Then, we derive the SNR_{req} from link-level simulations. After that, we translate the link-level results into system-level results using the capacity evaluation procedure introduced in section III-B. Finally, we calculate the number of constraints required by each detection mode. In Fig. 2, we provide the total throughput versus the number of constraints for the different mode assignments. It is seen that some detection modes, plotted with circles, perform worst than less complex modes. Indeed, even though the TR/D, R/D, D and D/H modes are able to effectively suppress 8PSK interference despite the channel estimation errors, their performance suffers from noise enhancement. The reason is that the noise and residual interference components[2] in the received signal are also being scaled by the combiner. This has been shown to result in greater noise and residual interference power. It is therefore inefficient to apply TR/D, R/D, D or D/H (complex modes) in an environment with accurate channel estimation where they do not significantly outperform modes with lower complexity. However, the R/H and H modes are more robust to the data estimation error, which is larger with high-order modulation (8PSK). Therefore, they outperform TR, TR/R and R despite noise enhancement. Fig. 2 also confirms that hybrid ISR provides a wider range of performance/complexity tradeoffs. Indeed, we can select one of the five detection modes plotted with squares: TR, TR/R, R, R/H and H compared to only three canonic detection modes TR, R and H. In wireless communication systems, there is a practical limit to the number of processing operations that can physically be supported. Taking into consideration the complexity limit, we choose the multi-user detection mode that maximizes the total throughput of the system. This work hence provides an analytical tool for a reliable, quick and efficient design of hybrid multi-user detection strategy in multi-rate CDMA transmission.

REFERENCES

[1] S. Affes, H. Hansen, and P. Mermelstein, "Interference subspace rejection : a framework for multiuser detection in wideband CDMA", *IEEE J. Select. Areas in Comm.*, vol. 20, no. 2, pp. 287-302, Feb. 2002.

[2] B. Smida, S. Affes, and P. Mermelstein, "Hybrid interference subspace rejection for multi-rate WCDMA", *Proc. of 22nd Biennial Symposium on Communications*, Queen's University, Kingston, Canada, pp. 143-145, May 31-June 3, 2004.

[3] H. Hansen, S. Affes , and P. Mermelstein, "Performance analysis of interference subspace rejection", submitted to *IEEE Trans. on Communications*, under review.

[4] A. Abrardo and D. Sennati,"On the analytical evaluation of closed-loop power-control error statistics in DS-CDMA cellular systems", *IEEE Transactions on Vehicular Technology*, vol. 49, no. 6, pp. 2071-2080, Nov. 2000.

[5] K. Cheikhrouhou, S. Affes, and P. Mermelstein, "Impact of synchronization on performance of enhanced array-receivers in wideband CDMA networks", *IEEE J. Select. Areas in Comm.*, vol. 19, no 12, pp. 2462-2476, Dec. 2001.

[2]The residual interference is due to wrong tentative data decisions, channel estimation errors and power control errors.

[6] S. Affes and P. Mermelstein, "Adaptive space-time processing for wireless CDMA", *Book Chapter, Adaptive Signal Processing: Application to Real-World Problems*, J. Benesty and A.H. Huang, Eds., Springer, Berlin, January 2003.

[7] T.S. Rappaport, *Wireless commmunications: principles* & *practice*, Prentice Hall PTR 1999.